

# Application of the Schwinger multichannel formulation to electron-impact excitation of the $B\ ^1\Sigma_u^+$ state of $H_2$

Thomas L. Gibson

*Department of Physics, Texas Tech University, Lubbock, Texas 79409*

Marco A. P. Lima\* and Vincent McKoy

*Arthur Amos Noyes Laboratory of Chemical Physics, California Institute of Technology, Pasadena, California 91125*

Winifred M. Huo<sup>†</sup>

*Radiation Laboratory, University of Notre Dame, Notre Dame, Indiana 46556*

(Received 12 September 1986)

In this paper we report cross sections for electron-impact excitation of the  $X\ ^1\Sigma_g^+ \rightarrow B\ ^1\Sigma_u^+$  transition in  $H_2$  for collision energies of 15, 20, and 30 eV. For this dipole-allowed transition with its associated long-range potential, the contributions of the more strongly scattered low-angular-momentum partial waves to the cross section were obtained from a two-state Schwinger multichannel calculation, and a modified Born-closure scheme was used to include the contributions from the remaining weakly scattered partial waves. Agreement between the calculated differential cross sections and available experimental data is encouraging.

## I. INTRODUCTION

Cross sections for the electronic excitation of molecules by low-energy electrons play an important role in several fields.<sup>1</sup> For example, these cross sections arise in the modeling of swarm and plasma-etching systems, of gas lasers, and of planetary atmospheres, and, more recently, in studies of adsorbate-substrate systems.<sup>2</sup> In spite of these needs, the availability of experimental data and of theoretical techniques for studying these cross sections is very limited. To date, most studies of electronic excitation of molecules by low-energy electrons have been carried out using low-order theories such as the Born and Ochkur-Rudge approximations,<sup>3,4</sup> the impact-parameter method,<sup>5</sup> and distorted-wave theories.<sup>6-8</sup> Although such theories can be computationally easy to apply, the available experimental data for electronic excitation of molecules are simply too limited and fragmentary to allow for a meaningful assessment of the limitations and applicability of these approximate theories.<sup>9,10</sup> Multichannel theories of these inelastic collisions have the firmest theoretical basis but are considerably more difficult to apply. Recently, however, several techniques which had previously been widely applied to electron-molecule collisions at the static-exchange level were extended to electronic excitation of  $H_2^+$ ,<sup>11-13</sup>  $H_2$ ,<sup>14-16</sup> and  $O_2$ .<sup>17</sup> Studies of the  $X\ ^1\Sigma_g^+ \rightarrow b\ ^3\Sigma_u^+$  excitation of  $H_2$  (Refs. 14-16) were particularly significant since they were carried out by applications of three different methods, namely, the Schwinger multichannel,<sup>14</sup> linear algebraic,<sup>15</sup> and  $R$  matrix,<sup>16</sup> all of which led to cross sections in substantial agreement with one another. These cross sections, obtained with only two open electronic channels, were also in reasonable agreement with experimental data. Furthermore, these results showed that correlation terms, which are included in the expansion of the scattering wave function so as to relax the orthogonality between bound and continuum orbitals,

affected the cross sections substantially.<sup>18</sup>

Prior to the present study, we have used the Schwinger multichannel method to calculate excitation cross sections for transitions from the ground electronic state to several triplet excited states of  $H_2$ .<sup>14,19</sup> Since these are dipole-forbidden transitions in which the coupling between the two states occurs through short-range exchange terms, it is usually not necessary to include a large number of partial waves for impact energies below 30 eV. Also, in these previous studies it has been possible to implement the Schwinger multichannel method entirely within an  $L^2$  basis. For dipole-allowed transitions such as the  $X\ ^1\Sigma_g^+ \rightarrow B\ ^1\Sigma_u^+$  transition in  $H_2$ , the long-range character of the dipolar coupling requires that a large number of partial waves be included to properly describe the scattering in the forward direction. If a full multichannel treatment is used to calculate dipole-allowed excitation cross sections, the need to include a large number of partial wave can add considerably to the computational effort. Further, in our noniterative implementation of the Schwinger method the initial set of basis functions must span the range of the interaction potential. Hence, dipole-allowed transitions may necessitate the inclusion of continuum functions, e.g., plane waves, in the variational basis from which the scattering wave function is constructed.

In this study we explore an expedient alternative to straightforward application of the full Schwinger multichannel method for use in computing dipole-allowed excitation cross sections. Although a large number of partial waves are needed to converge the small-angle scattering, above a certain minimum angular momentum  $l_m$ , the remaining partial waves are *weakly* scattered. Thus, if a *full* multichannel treatment of the scattering is used to calculate the partial-wave contribution to the differential cross sections,  $d\sigma/d\theta$ , up to  $l_m$ , the remaining terms can be obtained from a weak-scattering theory such as the

first Born approximation (FBA). For this dipole-allowed transition our procedure will hence be to use the Schwinger multichannel formulation<sup>20,21</sup> for the full scattering treatment and a modified Born-closure (BC) scheme to include contributions to the differential cross section from large-angular-momentum partial waves. Recent applications<sup>14,22–24</sup> of the multichannel Schwinger (SMC) method, in which the trial scattering wave functions were expanded in discrete basis functions, have shown that the procedure is very effective in describing the low-angular-momentum partial-wave contributions to the differential cross sections. In such applications, expansion of the trial scattering wave function in a large diffuse basis is clearly desirable. Finally, we note that the scheme of using a weak-scattering approximation to include contributions to the cross section from high angular momenta has been used in many applications, including collisions with polar molecules<sup>25–27</sup> and electron-impact excitation of dipole-allowed transitions.<sup>7,28</sup>

## II. THEORETICAL DEVELOPMENTS

Details of the Schwinger multichannel formulation used in these studies have been discussed elsewhere<sup>20,21</sup> and only a brief outline will be given here. The Hamiltonian for the collision system can be written as

$$H = (H_N + T_{N+1}) + V = H_0 + V, \quad (1)$$

where  $H_N$  is the target Hamiltonian,  $T_{N+1}$  is the kinetic-energy operator of the incident electron, and  $V$  is the interaction potential between the incident electron and the target, i.e.,

$$V = \sum_{i=1}^N \frac{1}{r_{i,N+1}} - \sum_{\alpha} \frac{Z_{\alpha}}{R_{\alpha,N+1}}. \quad (2)$$

In Eq. (2) the first and second terms are the electron-electron repulsion and electron-nuclei attraction, respectively. The total scattering wave function satisfies the Schrödinger equation

$$(E - H)\Psi_k = \hat{H}\Psi_k = 0. \quad (3)$$

To obtain a Schwinger variational principle for the multichannel scattering matrix associated with Eq. (3), we begin by introducing a projection operator  $P$  which defines the open-channel space in terms of the eigenfunctions of the target Hamiltonian  $H_N$ , i.e.,

$$P = \sum_m^{\text{open}} |\Phi_m(1,2,\dots,N)\rangle \langle \Phi_m(1,2,\dots,N)|, \quad (4)$$

and

$$H_N \Phi_m = E_m \Phi_m, \quad E - E_m > 0. \quad (5)$$

Note that the projector of Eq. (4) is different from the  $P$  operator of the Feshbach formalism.<sup>21,29</sup> With this operator we obtain a projected Lippmann-Schwinger equation:

$$P\Psi_k^{(+)} = P S_k + P G_0^{(+)} V \Psi_k^{(+)} \quad (6)$$

from

$$\Psi_k^{(+)} = S_k^{(+)} + G_0^{(+)} V \Psi_k^{(+)}, \quad (7)$$

where  $S_k$  is an eigenfunction of the unperturbed Hamiltonian  $H_0$ , i.e.,  $\Phi_m(1,\dots,N)e^{ik \cdot r_{N+1}}$ , and  $G_0^{(+)}$  in the Green's function associated with  $E - H_0$ . Note that the continuum states of the target molecule must be included in  $G_0^{(+)}$  in order to make the wave function  $\Psi_k^{(+)}$  on the left-hand side of Eq. (7) antisymmetric.<sup>30</sup>

We proceed by writing the Schrödinger equation in the form<sup>31</sup>

$$\hat{H}[aP\Psi_k^{(+)} + (1-aP)\Psi_k^{(+)}] = 0, \quad (8)$$

where  $a$  will be chosen to be  $N+1$ .<sup>20,31</sup> Insertion of Eq. (6) for  $P\Psi_k^{(+)}$ , followed by rearrangement of the resulting expression, gives the multichannel equation for  $\Psi_k^{(+)}$ ,

$$A^{(+)}\Psi_k^{(+)} = V S_k, \quad (9)$$

where

$$A^{(+)} = \frac{\hat{H}}{N+1} - \frac{P\hat{H} + \hat{H}P}{2} + \frac{PV + VP}{2} - V G_p^{(+)} V \quad (10)$$

and

$$G_p^{(+)} = \sum_m^{\text{open}} |\Phi_m\rangle g_m^{(+)}(r_{N+1}, r'_{N+1}) \langle \Phi_m|, \quad (11)$$

with

$$g_m^{(+)}(r, r') = -\frac{1}{2\pi} \frac{\exp(ik_m |r - r'|)}{|r - r'|}. \quad (12)$$

Based on Eq. (9) we can write a variational functional for the scattering amplitude

$$[f_{mn}] = -\frac{1}{2\pi} \frac{\langle \Psi_m^{(-)} | V | S_n \rangle \langle S_m | V | \Psi_n^{(+)} \rangle}{\langle \Psi_m^{(-)} | A^{(+)} | \Psi_n^{(+)} \rangle}. \quad (13)$$

Equation (15) is our multichannel extension of the usual Schwinger variational principle. Note that Eqs. (9) and (13) incorporate closed-channel effects without requiring the closed-channel Green's function which, in turn, would have to include the target continuum states. Expanding the variational scattering wave function in Eq. (13) in a basis of  $(N+1)$ -electron Slater determinants  $\Psi_i$ , the variational expression can be written as

$$\tilde{f}_{mn}^{\text{SMC}} = -\frac{1}{2\pi} \sum_{i,j} \langle S_m | V | \Psi_i \rangle (A^{-1})_{ij} \langle \Psi_j | V | S_n \rangle, \quad (14)$$

where  $(A^{-1})_{ij}$  is an element of the matrix inverse of  $A$ . In this formulation all configurations representing both open and closed channels are treated equivalently. Furthermore, the variational formulation is clearly based on the variation of the total wave function rather than of a specific scattering orbital.

Some important features of the variational principle of Eq. (14) are as follows. As in the original Schwinger principle,<sup>32</sup> an  $L^2$  expansion of the trial wave function is possible and will be assumed here. Furthermore, if the orbitals appearing in the  $(N+1)$ -electron Slater determinants,  $\Psi_i$ , in the expansion of the scattering wave function are chosen to be Cartesian Gaussian functions, all the matrix elements arising in Eq. (14), except those of  $V G_p^{(+)} V$ , can

be evaluated analytically for molecules of arbitrary geometry. The matrix elements associated with  $VG_p^{(+)}V$  can be obtained analytically if a large quadrature basis of Cartesian Gaussian functions is inserted around  $G_p^{(+)}$ .<sup>33,34</sup> We use this technique to obtain the principal-value contribution to the  $VG_p^{(+)}V$  matrix elements, but the on-shell contribution is obtained via insertion of a complete set of plane waves around  $G_p^{(+)}$ . This procedure results in an  $S$  matrix that is very nearly unitary without resorting to large Cartesian Gaussian insertion basis sets.<sup>24</sup>

Equation (13) provides an analytical approximation to the full scattering amplitude in the body frame. To obtain the differential cross section, we expand  $\hat{f}^{\text{SMC}}(\mathbf{k}_m, \mathbf{k}_n)$  in partial waves and make the requisite transformation to express the scattering amplitude in terms of the laboratory frame angles  $\hat{k}'_m$ , denoted by  $(\theta', \phi')$ . This partial-wave decomposition is carried out via a Gauss-Legendre quadrature.<sup>35</sup> The random orientation of the target molecule is accounted for by explicitly averaging over the incident (body-frame) angles  $\hat{k}_n$ , viz.,

$$\sigma^{\text{SMC}}(\theta', \phi'; k_m, k_n) = \frac{1}{4\pi} \frac{k_m}{k_n} \int d\hat{k}_n |f^{\text{SMC}}(\mathbf{k}'_m, \mathbf{k}_n)|^2. \quad (15)$$

Finally, the physical cross section  $\sigma^{\text{SMC}}(\theta')$  is obtained by averaging over the azimuthal angle  $\phi'$  and performing the appropriate average over initial and sum over final spin states for the transition of interest.

The cross section described above includes contributions from a finite number of angular momenta because the partial-wave decomposition of the scattering amplitude is truncated at some finite body-frame value  $(l_{\text{max}}, |m_{\text{max}}|)$  denoted by  $l_m$ . This value of  $l_{\text{max}}$  is, in turn, determined by the size of the Gauss-Legendre quadrature used in calculating the body-frame full scattering amplitudes for various plane-wave orientations. When the transition potential contains long-range moments, such as in dipole-allowed excitations, the number of partial waves required to converge  $\sigma^{\text{SMC}}(\theta')$  in the forward direction can be quite large. However, above a certain value of  $l_m$ , the contributions from high-angular-momentum partial waves can be included by means of a weak-scattering theory such as the first Born approximation. Furthermore, the FBA differential cross section  $\sigma^{\text{FBA}}(\theta')$  can be obtained in closed form<sup>7,33</sup> without resorting to a partial-wave expansion. Thus, within the FBA,  $\sigma^{\text{FBA}}(\theta')$  contains contributions from all angular momenta. Hence, our Born closure differential cross section  $\sigma^{\text{BC}}(\theta')$  is given by

$$\sigma^{\text{BC}}(\theta') = \sigma^{\text{FBA}}(\theta') + \Delta\sigma(\theta'), \quad (16)$$

where

$$\Delta\sigma(\theta') = [\sigma^{\text{SMC}}(\theta') - \sigma^{\text{FBA}}_{\text{FE}}(\theta')]. \quad (17)$$

In Eq. (17)  $\sigma^{\text{FBA}}_{\text{FE}}(\theta')$  is obtained from a finite expansion containing exactly the same number of partial waves as  $\sigma^{\text{SMC}}(\theta')$ . Thus, for angular momenta below  $l_m$ , contributions to  $\sigma^{\text{BC}}(\theta')$  are obtained from the Schwinger variational calculation, while the first Born approximation is used to include contributions to the cross section above

$l_m$ . The criterion<sup>27</sup> for the validity of Eq. (16) is that above  $l_m$  the contributions to  $\Delta\sigma$  are zero, i.e.,  $\Delta\sigma$  is converged.

In Sec. III we will discuss the results of an application of this procedure to the  $X^1\Sigma_g^+ \rightarrow B^1\Sigma_u^+$  transition in  $\text{H}_2$ . An alternative to this Born-closure approach would be to explicitly include plane waves in the expansion of the trial scattering wave function. It can be shown that,<sup>33</sup> with plane waves and Cartesian Gaussian functions in the expansion of the trial scattering function, all the matrix elements arising in the variational expression, Eq. (14), can still be evaluated analytically. This alternative remains to be tested.

### III. PROCEDURES AND RESULTS

We have used this multichannel Schwinger formulation and Born-closure procedure to study the differential cross sections for the  $X^1\Sigma_g^+ \rightarrow B^1\Sigma_u^+$  transition in  $\text{H}_2$  for electron-impact energies of 15, 20, and 30 eV. This application should be a reasonable test of our proposed procedure since the measured differential cross sections are quite strongly peaked in the forward direction for these energies while the cross sections obtained with a large discrete basis in the Schwinger variational expression are not. Measured cross sections<sup>36,37</sup> and results of other studies<sup>7,28</sup> are also available for comparison.

In these studies we include only two open channels and neglect closed channels. The cross sections are calculated within the framework of the fixed nuclei and Franck-Condon approximations. The nuclei are held fixed at the ground-state equilibrium value of  $1.4003a_0$  and the dependence of the electronic scattering amplitude on internuclear distance is neglected. The rotational levels are treated as degenerate and the physical cross section is averaged over all molecular orientations. The fixed-nuclei cross sections reported here thus correspond to the full band system, i.e., summed over all final vibrational levels. Unless otherwise stated, atomic units are used throughout.

For the ground electronic state we used a self-consistent-field (SCF) wave function obtained with a  $6s6p$  Cartesian Gaussian basis on the nuclei and a  $4s4p$  basis at the midpoint. These basis functions are shown in Table I. For the  $B^1\Sigma_u^+(1\sigma_g 1\sigma_u)$  state we made the frozen-core approximation and obtained the  $1\sigma_u$  orbital by diagonalizing the  $V_{N-1}$  potential of the  $1\sigma_g$  core in the SCF basis. The resulting vertical excitation energy is 12.73 eV. The entire set of "improved virtual orbitals" (IVO's) obtained in this diagonalization was augmented by  $6d_{xy}$  Gaussian functions. These  $d_{xy}$  functions are needed to expand the  $^2\Delta$  trial scattering functions. This expanded basis was then used to construct the  $(N+1)$ -electron scattering wave function, including the appropriate correlation terms required to relax the orthogonality constraint between the scattering and bound orbitals. Contributions to the body-frame scattering amplitudes from  $^2\Sigma_g, ^2\Sigma_u, ^2\Pi_u, ^2\Pi_g, ^2\Delta_g$ , and  $^2\Delta_u$  symmetries were included.

In these studies we chose  $l_m$  such that the contributions from the body frame  $^2\Sigma_g, ^2\Sigma_u, ^2\Pi_u, ^2\Pi_g, ^2\Delta_g$ , and  $^2\Delta_u$  scattering amplitudes with  $l \leq 5$  were obtained from a Schwinger variational calculation. Scattering amplitudes

TABLE I. Cartesian Gaussian basis sets, defined as  $\chi_{lmn} = N_{lmn}(x - A_x)^l(y - A_y)^m(z - A_z)^n \exp(-\alpha |\mathbf{r} - \mathbf{A}|^2)$ , where  $\mathbf{A}$  locates the Gaussian center. Basis sets used for the ground and excited states of  $\text{H}_2$ , in the expansion of the trial scattering wave functions, and in the insertion quadrature in  $VG_p^{(+)}V$ .

Center and type	Exponential
$H, 6s$	48.4479, 7.283 46, 1.651 39, 0.462 447, 0.145 885, 0.07
$H, 6p$	4.5, 1.5, 0.5, 0.25, 0.125, 0.031 25
Midpoint, $4s$	0.25, 0.05, 0.01, 0.002
Midpoint, $4p$	0.8, 0.2, 0.0625, 0.007 812 5
$H, 6d_{xy}^a$	4.5, 1.5, 0.5, 0.25, 0.125, 0.031 25

<sup>a</sup>Additional functions to expand the  $^2\Delta$  scattering wave functions.

of these symmetries are the ones that can be determined from an  $8 \times 8$  Gauss-Legendre quadrature for the full scattering amplitudes. The contributions to  $\sigma^{\text{BC}}(\theta')$  from partial waves with  $l \geq 6$  and  $|m| \geq 3$  were included via the first Born approximation. This choice of  $l_m$  is sufficient to converge  $\Delta\sigma$  of Eq. (17) at 15 eV. However, at 20 and 30 eV  $\Delta\sigma(\theta')$  is not fully converged for this choice of  $l_m$ , particularly for scattering angles between  $30^\circ$  and  $50^\circ$ . At this stage, instead of resorting to the considerably more extensive Schwinger calculations that would be required in extracting higher partial-wave amplitudes from the Schwinger amplitudes with the accuracy needed to converge  $\Delta\sigma(\theta')$  in this range of  $\theta'$  at these energies, we chose to use the following simple interpolation procedure. For the differential cross section at 20 and 30 eV, we take  $\sigma^{\text{BC}}(\theta')$  for  $\theta'$  between  $0^\circ$  and  $20^\circ$  and then use a cubic

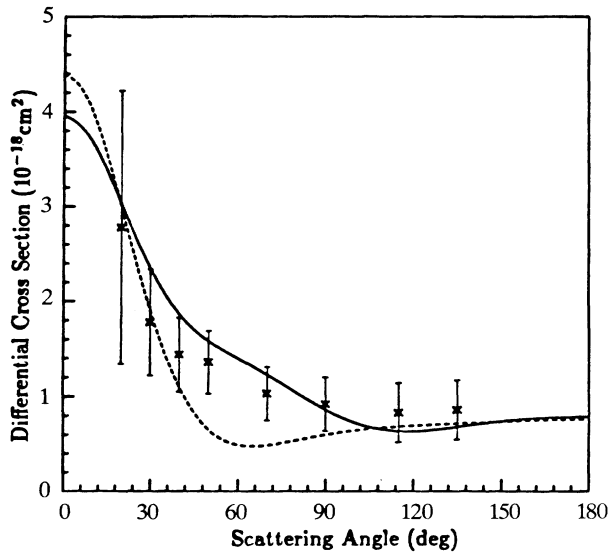


FIG. 1. Differential cross sections (DCS's) for the  $X^1\Sigma_g^+ \rightarrow B^1\Sigma_u^+$  transition at 15 eV: —, present results; — —, distorted-wave results of Ref. 7;  $\times$ , experimental results of Ref. 36.

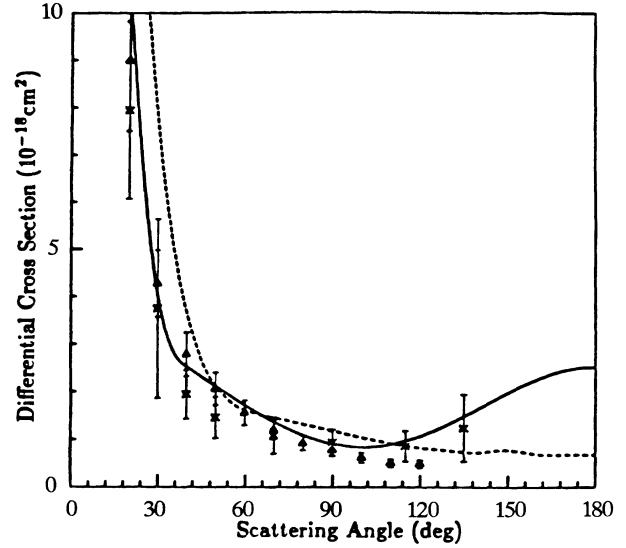


FIG. 2. DCS's for the  $X^1\Sigma_g^+ \rightarrow B^1\Sigma_u^+$  transition at 20 eV: —, present results; — —, distorted-wave results of Ref. 6;  $\times$  and  $\Delta$ , experimental results of Refs. 36 and 37, respectively.

spline interpolation to smoothly join the differential cross section onto  $\sigma^{\text{SMC}}(\theta')$  at  $\theta' = 40^\circ$  and  $50^\circ$ , respectively.

In Fig. 1 we show our calculated differential cross sections for the  $X^1\Sigma_g^+ \rightarrow B^1\Sigma_u^+$  excitation at 15 eV impact energy along with the distorted-wave Born-closure results of Ref. 7 and the experimental data of Srivastava and Jensen.<sup>36</sup> The agreement between our Born-closure cross sections and the measured data is very satisfactory at this energy. Although not shown in Fig. 1, the forward peaking in the calculated cross sections is not present in the cross sections derived solely from the Schwinger variational principle, i.e., without Born closure.

Figures 2 and 3 show our calculated differential cross

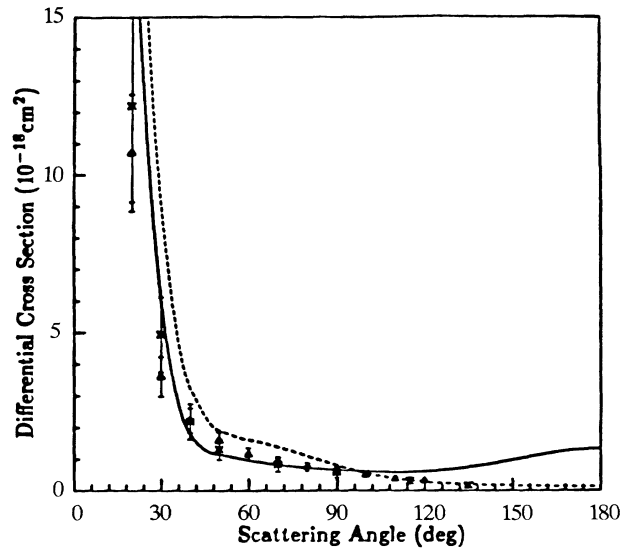


FIG. 3. DCS's for the  $X^1\Sigma_g^+ \rightarrow B^1\Sigma_u^+$  transition at 30 eV: —, present results; — —, distorted-wave results of Ref. 7;  $\times$  and  $\Delta$ , experimental results of Refs. 36 and 37.

TABLE II. Integral cross sections for the  $X^1\Sigma_g^+ \rightarrow B^1\Sigma_u^+$  excitation in  $H_2$  ( $10^{-17}$  cm<sup>2</sup>).

Impact energy (eV)	DW <sup>a</sup>	CC <sup>b</sup>	SMC <sup>c</sup>	FBA <sup>d</sup>	Expt. <sup>e</sup>	Expt. <sup>f</sup>
15	1.05		1.41	4.12	1.7±0.5	
20	3.09		2.66	6.31	2.5±0.7	2.1±0.4
25	4.12	4.31		6.90		
30	4.46		4.0	7.0	2.4±0.7	2.4±0.5

<sup>a</sup>Distorted-wave Born-closure results of Ref. 7.<sup>b</sup>Two-state close-coupling Born-closure results of Ref. 28.<sup>c</sup>Present results.<sup>d</sup>First Born results of this work.<sup>e</sup>Experimental data of Ref. 36.<sup>f</sup>Experimental data of Ref. 37.

sections at 20 and 30 eV along with the distorted-wave Born-closure results<sup>7</sup> and the experimental data of Refs. 36 and 37. The overall agreement between our calculated cross sections and the measured values is quite good for all angles. For higher angles at 20 eV our cross sections show a slight backward peaking beyond 120°, a feature seen in the data of Srivastava and Jensen<sup>36</sup> but not in those of Ref. 37. Measurements of these cross sections at these larger angles, as well as at small angles, are difficult, in general, and calculated differential cross sections, particularly in the experimentally inaccessible region beyond 120°, would clearly be very useful in any extrapolation of experimental data into these angular regions. Note that the distorted-wave Born-closure cross sections, particularly at 20 eV, continue to fall off beyond 120°, in contrast to the results of the present two-state calculation.

Our integral excitation cross sections are listed in Table II along with available experimental data and the results of the distorted-wave calculations of Fliflet and McKoy<sup>7</sup> and of the two-state close-coupling studies of Chung and Lin.<sup>28</sup> The agreement between our calculated two-state cross sections and the experimental data at 15 and 20 eV is quite good. The large uncertainties in the measured cross sections at these energies come primarily from the experimentally difficult low-angle region and from extrapolation procedures used in obtaining integral cross sections from differential data over a restricted angular range. At 30 eV impact energy our calculated cross section, and its trend with energy, agrees poorly with the measured values. This may be due to the inherent limitations of a two-state calculation as the collision energy increases and/or greater uncertainties in the extrapolation procedure used in deriving the experimental cross section at this higher energy. This serves to emphasize the need for reporting differential excitation cross sections in theoretical studies of electron collisions. For example, the differential cross sections shown in Figs. 1–3 provide a more meaningful physical comparison among the theoretical procedures and the experimental data. The distorted-wave results<sup>7</sup> in Table II are quite similar to the present two-state Born-closure cross sections. Some of the differences between these cross sections arise from the fact that in the distorted-wave calculations<sup>7</sup> an explicit sum over discrete vibrational levels with appropriate

Franck-Condon factors and final-state momenta was used. The apparent agreement between the two-state close-coupling results of Chung and Lin,<sup>28</sup> obtained with orthogonality constraints between bound and continuum orbitals, and our interpolated cross sections at 25 eV, is reasonable. The corresponding cross sections for the  $X^1\Sigma_g^+ \rightarrow b^3\Sigma_u^+$  transition in  $H_2$  showed significantly larger differences. Finally, we note that both the distorted-wave<sup>7</sup> and close-coupling results<sup>28</sup> in Table II also utilized some form of Born-closure scheme to obtain the higher-partial-wave contributions to the cross sections.

#### IV. CONCLUSIONS

In this paper we have presented cross sections for electron-impact excitation of the  $X^1\Sigma_g^+ \rightarrow B^1\Sigma_u^+$  transition in  $H_2$  at collision energies of 15, 20, and 30 eV. For this dipole-allowed transition with its long-range transition potential, these results were obtained from a Schwinger multichannel calculation and a Born-closure procedure. The Schwinger multichannel calculation was carried out with a discrete basis expansion of the trial scattering wave function and was used to obtain the contribution to the cross section from the strongly scattered low-angular-momentum partial waves. The Born-closure scheme provided the contributions from the remaining weakly scattered partial waves. The agreement between the calculation differential cross section and available experimental data at these impact energies is encouraging.

#### ACKNOWLEDGMENTS

This material is based upon research supported by the National Science Foundation under Grant No. PHY-82-13992 and by NASA-Ames Cooperative Agreement No. NCC2-319. One of us (M.A.P.L.) acknowledges financial support from the Comissão Nacional de Energia Nuclear (CNEN), Rio de Janeiro, Brazil, and from Fundação de Amparo à Pesquisa do Estado de São Paulo, São Paulo, Brazil. The research of W.M.H. is supported by the National Aeronautics and Space Administration through NASA-Ames Cooperative Agreement No. NCC2-147.

- \*Permanent address: Instituto de Estudos Avançados, Centro Técnico Aeroespacial, 12200 São José dos Campos, São Paulo, Brazil.
- †Mailing address: NASA Ames Research Center, MS 230-3, Moffett Field, CA 94035.
- <sup>1</sup>See, for example, S. C. Brown, *Electron-Molecule Scattering* (Wiley, New York, 1979).
- <sup>2</sup>Ph. Avouris and J. E. Demuth, *Annu. Rev. Phys. Chem.* **34**, 49 (1984).
- <sup>3</sup>S. Chung, C. C. Lin, and E. T. P. Lee, *Phys. Rev. A* **12**, 1340 (1975).
- <sup>4</sup>D. C. Cartwright and A. Kuppermann, *Phys. Rev.* **163**, 86 (1967).
- <sup>5</sup>A. U. Hazi, *Phys. Rev. A* **23**, 2232 (1981).
- <sup>6</sup>T. N. Rescigno, C. W. McCurdy, Jr., and V. McKoy, *J. Phys. B* **7**, 2396 (1974).
- <sup>7</sup>A. W. Fliflet and V. McKoy, *Phys. Rev. A* **21**, 1863 (1980).
- <sup>8</sup>M.-T. Lee and V. McKoy, *Phys. Rev. A* **28**, 697 (1983).
- <sup>9</sup>See, for example, D. C. Cartwright, A. Chutjian, S. Trajmar, and W. Williams, *Phys. Rev. A* **16**, 1013 (1977).
- <sup>10</sup>S. Trajmar, D. F. Register, and A. Chutjian, *Phys. Rep.* **97**, 219 (1983).
- <sup>11</sup>J. Tennyson, C. J. Noble, and S. Salvini, *J. Phys. B* **17**, 905 (1984).
- <sup>12</sup>J. Tennyson and C. J. Noble, *J. Phys. B* **18**, 155 (1985).
- <sup>13</sup>B. I. Schneider and L. A. Collins, *Phys. Rev. A* **28**, 166 (1983).
- <sup>14</sup>M. A. P. Lima, T. L. Gibson, W. M. Huo, and V. McKoy, *J. Phys. B* **18**, L865 (1985).
- <sup>15</sup>B. I. Schneider and L. A. Collins, *J. Phys. B* **18**, L857 (1985).
- <sup>16</sup>K. L. Baluja, C. J. Noble, and J. Tennyson, *J. Phys. B* **18**, L851 (1985).
- <sup>17</sup>C. J. Noble and P. J. Burke, *J. Phys. B* **19**, L19 (1986).
- <sup>18</sup>For results of earlier two-state close-coupling calculations of the  $X^1\Sigma_g^+ \rightarrow B^1\Sigma_u^+$  cross sections with the orthogonality constraint on bound and continuum orbitals, see Ref. 28.
- <sup>19</sup>M. A. P. Lima, W. M. Huo, and V. McKoy (unpublished).
- <sup>20</sup>K. Takatsuka and V. McKoy, *Phys. Rev. A* **24**, 2473 (1981).
- <sup>21</sup>K. Takatsuka and V. McKoy, *Phys. Rev. A* **30**, 1734 (1984).
- <sup>22</sup>L. M. Brescansin, M. A. P. Lima, T. L. Gibson, V. McKoy, and W. M. Huo, *J. Chem. Phys.* **85**, 1854 (1986).
- <sup>23</sup>M. A. P. Lima, T. L. Gibson, W. M. Huo, and V. McKoy, *Phys. Rev. A* **32**, 2696 (1985).
- <sup>24</sup>W. M. Huo, T. L. Gibson, M. A. P. Lima, and V. McKoy (unpublished).
- <sup>25</sup>O. H. Crawford and A. Dalgarno, *J. Phys. B* **4**, 494 (1971).
- <sup>26</sup>L. A. Collins and D. W. Norcross, *Phys. Rev. A* **18**, 467 (1978).
- <sup>27</sup>D. W. Norcross and N. T. Padial, *Phys. Rev. A* **25**, 226 (1982).
- <sup>28</sup>S. Chung and C. C. Lin, *Phys. Rev. A* **17**, 1874 (1978).
- <sup>29</sup>H. Feshbach, *Ann. Phys. (N.Y.)* **19**, 287 (1962).
- <sup>30</sup>S. Geltman, *Topics in Atomic Collision Theory* (Academic, New York, 1969), p. 99.
- <sup>31</sup>See, also, M. A. P. Lima and V. McKoy (unpublished).
- <sup>32</sup>B. A. Lippmann and J. Schwinger, *Phys. Rev.* **79**, 469 (1950).
- <sup>33</sup>D. K. Watson and V. McKoy, *Phys. Rev. A* **20**, 1474 (1979); D. K. Watson, R. R. Lucchese, V. McKoy, and T. N. Rescigno, *ibid.* **21**, 738 (1980).
- <sup>34</sup>N. S. Ostlund, *Chem. Phys. Lett.* **34**, 419 (1975).
- <sup>35</sup>M. A. P. Lima, T. L. Gibson, K. Takatsuka, and V. McKoy, *Phys. Rev. A* **30**, 1741 (1984).
- <sup>36</sup>S. K. Srivastava and S. Jensen, *J. Phys. B* **10**, 3341 (1977). Here we use the renormalized results as recommended in Ref. 10.
- <sup>37</sup>M. A. Khakoo and S. Trajmar, *Phys. Rev. A* **34**, 146 (1986).